Effect of additional monopole electron ejections on the final ion charge spectra following the cascade decay of electron vacancies in the gold atom

© *A.P. Chaynikov, A.G. Kochur, A.I. Dudenko, V.A. Yavna*

Rostov State Transport University,
344038 Rostov-on-Don, Russia

e-mail: chaynikov.a.p@gmail.com

The probabilities of the formation of final ions produced by the cascade decays of vacancies in the K-, L-, M-, N- and O-shells of the gold atom are calculated. Simulation of the cascade decays of vacancies is performed by direct construction and analysis of decay trees using branching ratios and transition energies calculated in the Pauli−Fock approximation for multivacancy electron configurations arising in the course of the cascade decay. Accounting for additional monopole ejections of electrons (shake-off) accompanying the cascade transitions leads to a slight increase in the average charges of the final ions, by $0.15-0.23e$. The largest relative increase in the calculated average charges of the final ions (by $3.6-3.9\%$) is observed upon the cascade decay of vacancies in $4p_{3/2}$-, $4d_{3/2}$-, and $4d_{5/2}$-subshells, and the smallest (by 0.8%) occurs in the decay of $4f$-vacancy. Despite insignificant changes in the average ion charges, the structure of the charge spectra in some cases changes noticeably enough when additional electron ejections are taken into account. It is expected that in simulation of the cascade energy reemission processes when heavy atoms are used as radiosensitizers, the effect of accounting for shake-off processes will be insignificant.

Keywords: cascade decay of vacancies, charge spectra of cascade ions, monopole multiple ionization, shake-off, radiosensitization.

Introduction

Creation of a vacancy in an inner electron shell of an atom triggers the process of the cascade decay of the vacancy. The decay of a vacancy in the inner electron shell of an atom is, as a rule, a sequence of radiative and non-radiative transitions, each of which is accompanied by the emission of a photon (radiative transitions) or an electron (non-radiative Auger, Coster−Kronig and super-Coster−Kronig transitions). In the case of the decay of a vacancy in the deep shell of a heavy atom, the cascade may contain a significant number of non-radiative transitions, which leads to the formation of final ions with large charges.

In the pioneering works of Krause and Carlson with coworkers [1–6], the probabilities of formation of final ions (charge spectra) were measured and calculated for the first time upon the decay of vacancies in rare gas atoms. Rare gases continue being the subject of attention of researchers in theoretical description of cascade decays of vacancies, and calculation of the final ions charge spectra [7–23]. Charge spectra upon the decay of vacancies in the inner shells of the iron atom were calculated in [24–27]. The authors of [28] calculated cascade decays in the magnesium atom and isoelectronic ion Fe^{14+}. In [29] the charge spectrum was calculated for the decay of $1s$-vacancy in the Mg atom. In [30], the cascade charge spectra are calculated

for the decay of vacancies in Ne, Mg, Si, S, Ar atoms, and their isonuclear ions. Charge spectra on the decay of $4d$-vacancies in atoms of the rare earth metals Ce, Pr, Nd, Pm, Sm, Eu, and Gd were calculated in [31]. El-Shemi et al. [32–35] carried out systematic calculations of charge spectra upon the decay of inner-shell vacancies of a large number of atoms up to mercury.

During the creation of an inner-shell vacancy and during cascade transitions, additional monopole electron ejections are possible due to a sudden change in the atomic potential. In the English-language literature such processes are called shake-off (SO) processes [36–39]. The effect of SO processes on the charge spectra at cascade decays of vacancies in deep electron shells of atoms is taken into account in the calculations performed in refs. [11–14,16,18,22,32,33,35]. It is shown that in many cases, especially during the decay of vacancies in light atoms, the effect of SO processes on the charge spectra of final ions can be significant: it leads to an increase in the relative probabilities of formation of ions with large charges and improves the agreement between the calculated charge spectra and experiment.

In the theoretical description of cascade decays of vacancies, the so-called decay tree should be constructed. The branching points of the decay tree are the initial configuration of an atom with a deep vacancy, and all subsequent ionic configurations that may appear during the

development of the cascade. The branches of the decay tree are cascade electron transitions connecting the branching points. Accounting for the SO processes caused by the change of potential during cascade transitions significantly complicates the decay tree greatly increasing the number of branches. Therefore, accounting for such processes is a time consuming task. In [40], charge spectra of final ions are calculated in cascade decays of vacancies in *K*-, *L*-, *M*-, *N*- and *O*-shells of the gold atom without taking into account additional SO processes. Wherein it was suggested that in case of cascades with deep initial vacancies, the effect of additional monopole emissions on final ions charge spectra should not be large since the vast majority of cascade transitions occur in multiply ionized atoms, and the relative changes of potential caused by the cascade transitions will be small. The aim of this work is a direct calculation of the charge spectra of final ions on the decay of vacancies in the deep electron shells of the gold atom taking into account additional SO ejections.

Among the theoretical approaches to the description of cascade decays of vacancies, the Monte−Carlo method is the most widespread. Within this method, the same numerical experiment is repeated many times: the decay of an initial vacancy is simulated with a random choice of the next decay branch at each subsequent branching point. In this case, the number of trials that ended with the formation of final ions of each charge is counted, and the probability of their formation is calculated in accordance with the frequentist probability definition.

An alternative method based on the direct construction and analysis of an entire decay tree was previously used only for the qualitative analysis of rather simple cascades, for example, the decay of the 1*s*-vacancy in the argon atom [41]. In [13,14], the method of direct construction of a complete tree of the cascade decay was implemented numerically which allowed to apply it to a quantitative description of rather complex cascades, such as 1*s* cascades in krypton and xenon [13,14], iron [25] and gold [40]. The calculations of this work were carried out by the method of direct construction and analysis of decay trees.

Method of calculation

The method for calculating the probabilities of formation of cascade ions by constructing a complete decay tree of vacancy decay is described in detail in refs. [13,14]. In this section, we give a brief description of the method and discuss of the features that are important in describing cascade decays of vacancies in the deep shells of heavy atoms.

Let $C^{(0)} = \text{Au}[nl_j^{-1}]$ be the electron configuration of the gold ion with the initial vacancy in the deep inner subshell nl_j. This is the first branching point in the decay tree. At the first step of the cascade decay, the $C^{(0)}$ configuration, through various energy-allowed radiative and/or non-radiative transitions, can decay into configurations from

the $\{C_i^{(1)}\}$ set, which forms the first generation of the cascade ionic configurations. If any configurations from the $\{C_i^{(1)}\}$ set have inner-shell vacancies, they decay further, forming the next generation of ionic configurations $\{C_j^{(2)}\}$, etc. This process goes on until none of the *n*-th generation configurations $\{C_k^{(n)}\}$ can decay further, having vacancies only in the outermost electron subshells.

The key characteristics of each $C_i^{(m)}$ branching point in the decay tree is the relative probabilities of transitions to next-generation states $C_j^{(m+1)}$, also called branching ratios:

$$\chi\left(C_i^{(m)} \rightarrow C_j^{(m+1)}\right) = \frac{\Gamma\left(C_i^{(m)} \rightarrow C_j^{(m+1)}\right)}{\sum\limits_k \left(C_i^{(m)} \rightarrow C_k^{(m+1)}\right)}. \qquad (1)$$

Here Γ — partial widths of transitions, and the summation is performed over all energetically allowed radiative and non-radiative transitions.

When the processes of additional monopole ejections are taken into account, to the main branches of the decay tree corresponding to the electron transitions $T_{ij} = C_i \rightarrow C_j$ (hereinafter, the indices of the decay steps are omitted), additional SO-branches $T_{ij}^{\text{SO}}(nl) = C_i \rightarrow C_j^{\text{SO}}(nl^{-1})$ are added, in the final configurations of which there are additional vacancies in the outer subshells nl. Each of the additional branches has a branching ratio

$$\chi^{\text{SO}}(C_i \rightarrow C_j) = \chi(C_i \rightarrow C_j)P(T_{ij}, nl), \qquad (2)$$

where $P(T_{ij}, nl)$ — the probability of a monopole ejection of nl electron caused by a change in the potential of the atomic core due to the T_{ij} transition, and the branching ratio is determined by the relation (1). Accordingly, the branching ratio for a transition without an additional ejection is modified:

$$\chi'(C_i \rightarrow C_j) = \chi(C_i \rightarrow C_j)[1 - \sum_{nl} P(T_{ij}, nl)]. \qquad (3)$$

Let the decay tree be completely built. Non-decaying final ionic configurations correspond to the ions Au^{q+} with certain charge q. Such $C(q)$ configurations can be detected at many decay steps, and then the probability $P(q)$ of the formation of the final ion Au^{q+} is equal to the sum of the probabilities of the formation of $C(q)$ ionic configurations for different decay pathways consisting of successive branches leading from $C^{(0)}$ to $C(q)$. In turn, for each particular pathway $C^{(0)} \rightarrow C_i^{(1)} \rightarrow \ldots C(q)$, the probability of formation of the final configuration $C(q)$ is equal to the product of the branching ratios of all branches (transitions) between $C^{(0)}$ and $C(q)$.

In the gold atom, most of the nl levels with $l \neq 0$ are strongly split by the spin-orbit interaction, which opens up the opportunity of intense Coster-Kronig transitions. In this regard, the initial neutral configuration of the gold atom is taken as $\text{Au}[0] = 1s^2 2s^2 2p_{1/2}^2 2p_{3/2}^4 3s^2 3p_{1/2}^2 3p_{3/2}^4 3d_{3/2}^4 3d_{5/2}^6 4s^2$

$4p_{1/2}^2 4p_{3/2}^4 4d_{3/2}^4 4d_{5/2}^6 4f^{14} 5s^2 5p_{1/2}^2 5p_{3/2}^4 5d^{10} 6s^1$. In case of $4f$- and $5d$-subshells, the spin-orbit splitting is much smaller than the splitting associated with the electrostatic interaction.

The radial parts of the wave functions of ions in various multivacancy cascade configurations are calculated in the Pauli−Fock (PF) [42] approximation without spin-orbit splitting, i.e. for spin-orbit-unsplit, „compressed", $\{nl_j^{N_{nlj}}\}$ configurations with occupation numbers $N_{nl} = N_{nl_{l-1/2}} + N_{nl_{l+1/2}}$. Meanwhile, the energies of the $\{nl_j^{N_{nlj}}\}$ configurations, taking into account spin-orbit splittings, were calculated using the total energies of the corresponding compressed $\{nl^{N_{nl}}\}$ PF configurations and calculated spin-orbit interaction constants. The total number of various ionic PF configurations that needed to be optimized in describing the cascade decays of vacancies in the gold atom was 162307.

The partial widths of the transitions in (1) essentially depend on the electron configuration of the ion from which the transition takes place. In order to take this effect into account, partial radiative widths per vacancy and one electron (γ_{ij}) and partial non-radiative widths per vacancy and one pair of electrons (γ_{ijk}) are introduced:

$$\gamma_{ij} = \frac{4}{3}\left(\frac{E_{ij}}{c}\right)^3 \frac{\max(l_i, l_j)}{2(2l_i+1)(2l_j+1)} R_{ij}^2, \qquad (4)$$

$$\gamma_{ijk} = \frac{\Gamma_{i-jk}^0}{N_{jk}^{\max}}, \qquad N_{jk}^{\max} = \begin{cases} N_j^{\max} N_k^{\max}, & j \neq k, \\ 0.5 N_j^{\max}(N_j^{\max}-1), & j = k. \end{cases} \qquad (5)$$

In (4) indices i and j denote the initial and final vacancies of the radiative $i-j$ transition, E_{ij} — the energy of the emitted photon, c — the speed of light in vacuum, $R_{ij} = \langle n_i l_i | r | n_j l_j \rangle$ – the radial part of the dipole transition probability amplitude (all quantities in the atomic system of units). In (5), the indices i and j, k denote the levels with the initial and final vacancies of the non-radiative $i-jk$ transition, Γ_{i-jk}^0 — the width of the $i-jk$ transition calculated in the configuration with one initial vacancy in the i subshell and completely filled subshells j and k. $N_{jk}^{\max}$ is equal to the number of ways in which a pair of electrons can be taken from completely filled subshells j, and k, $N_j^{\max}$ and $N_k^{\max}$ — maximal occupation numbers of subshells. For subshells $n_k l_k$ without spin-orbit splitting $N_k^{\max} = 4l_k + 2$, for spin-orbit-split subshells $n_k l_{kj_k}$, $N_k^{\max} = 2j_k + 1$. The partial widths of radiative Γ_{i-j}^0 and non-radiative Γ_{i-jk}^0 transitions in the gold atom for the case of single initial vacancies i^{-1} are calculated in the PF approximation and are given in [40].

As can be seen from (4), only electric dipole radiative transitions are taken into account in this study. Accounting for non-dipole transitions would make sense only for the decay of the deepest vacancies in *K*- and *L*-shells, where radiative decay channels predominate or are comparable in probability to non-radiative ones. However, non-dipole transitions make only a small contribution to the fluorescence yield for them [43]: 0.4% for shell *K*, 3.2% for L_1, 0.2% for L_2 and L_3. Thus, allowance for possible non-dipole transitions would not result in a noticeable change in the decay dynamics.

In case when the radiative transition $i-j$ occurs in an arbitrary multivacancy configuration C, and at least one of the subshells involved in the transition is not split by the spin-orbit interaction, the transition width is calculated by the formula

$$\Gamma_{i-j}(C) = N_i^v N_j \gamma_{ij}, \qquad (6)$$

where N_i^v — the number of vacancies in the subshell i, and N_j — the number of electrons in the subshell j before the transition. If both subshells involved in the transition are components of spin-doublets, then the expression for the transition width is

$$\Gamma\left(n_1 l_1 j_1^{N_1} n_2 l_2 j_2^{N_2} \to n_1 l_1 j_1^{N_1+1} n_2 l_2 j_2^{N_2-1}\right)$$

$$= 2(2j_1 + 1 - N_1) N_2 (2l_1 + 1)(2l_2 + 1)$$

$$\times \begin{Bmatrix} l_2 & j_2 & 1/2 \\ j_1 & l_1 & 1 \end{Bmatrix}^2 \gamma_{n_1 l_1 n_2 l_2}. \qquad (7)$$

The widths of non-radiative transitions $i-jk$ in an arbitrary configuration C of the ion are calculated as

$$\Gamma_{i-jk}(C) = N_i^v N_{jk} \gamma_{ijk}. \qquad (8)$$

Here N_i^v has the same meaning as in (6), and N_{jk} is the number of electron pairs that can be ejected from the j and k subshells which is expressed using the occupation numbers of subshells in the same way as in (5). The use of (6)−(8) allows to easily take into account the influence of the electronic configuration of the ion on the transition widths and branching ratios (1)−(3).

Let us note that strict calculation of the widths of non-radiative transitions in arbitrary ionic configurations is a complicated task [44–46] and is unthinkable when modeling complex cascades due to the huge number of different multivacancy ionic configurations generated by cascades. At the same time, the approximation (5), (8), used in this work and based on the widths of transitions involving completely filled electron subshells, quite adequately reproduces the change in the partial widths of transitions with a change in the electronic configuration of the decaying ion. It has been used many times before [13,14,47] and has led to the results comparing well with experiment.

Mirakhmedov and Parilis [9] pointed out that in the case of cascade decay of vacancies, some non-radiative transitions may turn out to be energetically forbidden in multivacancy intermediate ionic configurations generated by the cascade. Accounting for the forbiddance of such transitions is especially important in describing cascade decays of deep vacancies in heavy atoms, in which a large number of intermediate multivacancy ionic states are formed. In addition, as noted in [40], the forbiddance of the transition between the ionic configurations C_1 and C_2

cannot be considered as a sudden disappearance of the transition as soon as the average total energy E_{02} of the final configuration C_2 exceeds the energy E_{01} of the initial configuration C_1.

Indeed, both C_1, and C_2 — are complex multiplets that can overlap in energy. Then, even under the condition $E_{02} > E_{01}$, some components of the C_1 multiplet may still lie higher in energy than some components of the C_2 multiplet, and transitions between such components are possible. Then the transition $C_1 \rightarrow C_2$ is only partially forbidden. On the other hand, if the $C_1 \rightarrow C_2$ transition is formally allowed, i.e. if the condition $E_{02} < E_{01}$ is satisfied, with close E_{02} and E_{01}, some components of the C_1 multiplet may turn out to be lower in energy than some components of the C_2 multiplet, and the transitions between such states will be impossible. In other words, the $C_1 \rightarrow C_2$ transition is only partially allowed.

A rigorous calculation of the structure of all multiplets of initial and final states of all cascade transitions does not seem to be technically possible since the number of ionic configurations generated by cascades is very large. The method of global characteristics of spectra [48,49] is used to describe the energy structure of multiplets of multivacancy ionic configurations. The multiplet of the ionic configuration C is a set of states characterized by energies E_i and statistical weights g_i. When using the global characteristics of the spectra, the set of discrete components of the $\{E_i, g_i\}$ multiplet is approximated by the normal distribution of the probability density:

$$p(E, E_0, \sigma) = \frac{1}{\sqrt{2\pi\sigma^2}} \exp\left(-\frac{(E-E_0)^2}{2\sigma^2}\right). \quad (9)$$

The distribution center is determined by the relation

$$E_0 = \frac{\sum_i g_i E_i}{\sum_i g_i}, \qquad g_i = 2J_i + 1. \quad (10)$$

Here J_i is the quantum number of the total angular momentum. The distribution variance is

$$\sigma^2 = \frac{\sum_i g_i (E_i - E_0)^2}{\sum_i g_i}. \quad (11)$$

Distribution centers E_0 are the average energies of configurations calculated in this work directly for each ionic configuration formed during the cascade decay of a vacancy. Distribution variances are calculated for all ionic configurations from the known populations of electron subshells and electrostatic interaction integrals by the methods of refs. [48,49].

Consider the transition between multiplets of ionic configurations C_1 and C_2 represented by the distributions $p_1(E, E_{01}, \sigma_1)$ and $p_2(E, E_{02}, \sigma_2)$. The average transition

energy is

$$\langle E(C_1 \rightarrow C_2) \rangle$$

$$= \int_{-\infty}^{\infty} p_1(E_1, E_{01}, \sigma_1) dE_1 \int_{-\infty}^{E_1} (E_1 - E_2) p_2(E_2, E_{02}, \sigma_2) dE_2$$

$$= \frac{1}{2} \frac{\sqrt{2(\sigma_1^2 + \sigma_2^2)}}{\sqrt{\pi}} \exp\left(\frac{-(E_{01} - E_{02})^2}{2(\sigma_1^2 + \sigma_2^2)}\right)$$

$$+ \frac{E_{01} - E_{02}}{2}\left[1 + \mathrm{erf}\left(\frac{E_{01} - E_{02}}{\sqrt{2(\sigma_1^2 + \sigma_2^2)}}\right)\right]. \quad (12)$$

In the case of non-overlapping multiplets at $E_{01} > E_{02}$ the average transition energy is $\langle E(C_1 \rightarrow C_2)\rangle = E_{01} - E_{02}$. If the multiplets overlap is significant, i.e. difference $|E_{01} - E_{02}|$ is comparable to $\sqrt{2(\sigma_1^2 + \sigma_2^2)}$, then (12) takes into account only energy-allowed transitions between the multiplet components C_1 and C_2.

If the C_1 and C_2 multiplets overlap, then the partial width of the $C_1 \rightarrow C_2$ transition should also be corrected:

$$\Gamma^{corr}(C_1 \rightarrow C_2) = \alpha(E_{01}, \sigma_1, E_{02}, \sigma_2)\Gamma(C_1 \rightarrow C_2). \quad (13)$$

Here, the correction factor

$$\alpha(E_{01}, \sigma_1, E_{02}, \sigma_2) = \int_{-\infty}^{\infty} p_1(E_1, E_{01}, \sigma_1) dE_1$$

$$\times \int_{-\infty}^{E_1} p_2(E_2, E_{02}, \sigma_2) dE_2 = \frac{1}{2}\left[1 + \mathrm{erf}\left(\frac{E_{01} - E_{02}}{\sqrt{2(\sigma_1^2 + \sigma_2^2)}}\right)\right] \quad (14)$$

is equal to the fraction of states of the multiplet C_1, for which the transition to the multiplet states C_2 is energy allowed.

In [40] it is demonstrated that the exact calculation of the average energies of ionic configurations and allowance for multiplet overlap are critically important in calculating the probabilities of cascade ions formation. Thus, the calculation [40] of the average charge of final ions during the decay of $2s$ vacancy in the gold atom ($Z = 79$) gave a value of 9.81, while the average charge of final ions during the decay of $2s$ vacancy in a neighboring mercury atom ($Z = 80$), calculated in [32] without these effects, was 13.83. At that, a deliberately simplified calculation performed in [40] without taking into account the forbiddance of non-radiative transitions in multiply ionized configurations and without taking into account the overlap of multiplets gave a close value of the average charge of the final ions equal to 13.92.

The probabilities of additional electron ejections from nl-subshells $P(T_{ij}, nl)$, caused by a change of the atomic core potential as a result of the electron transition $T_{ij} = C_i \rightarrow C_j$,

are calculated in sudden approximation [36–39] by the equation

$$P(T_{ij}, nl) = kN_{nl}\left[1 - \langle nl(C_i)|nl(C_j)\rangle^2\right], \quad (15)$$

where $nl(C_i)$ and $nl(C_j)$ in the overlap integral are radial parts of outer subshell wave functions nl optimized in initial C_i and final C_j configurations of the transition, N_{nl} is the occupation number of nl subshell in initial configuration, k is a correction factor. When using in (15) the radial parts of self-consistent wave functions $k = 1$.

    In this work, as in earlier studies [13,14], the overlap integrals in (15) are calculated approximately using the analytical radial parts of atomic orbitals (AO) of the form

$$P_{nl}(r) = A_{nl}r^{l+1}\exp(-\beta_{nl}r), \quad (16)$$

where the factors A_{nl} and β_{nl} are determined by the normalization condition and the requirement that the AO's average radius calculated using (16):

$$\bar{r}_{nl} = \int\limits_0^\infty rP_{nl}^2(r)dr, \quad (17)$$

coincided with the average radius calculated using the radial part of the self-consistent AO.

    When using the AO radial parts (16), the overlap integrals in (15) are expressed analytically in terms of the average AO radii $nl(C_i)$ and $nl(C_j)$, calculated using self-consistent functions:

$$\langle nl(C_i)|nl(C_j)\rangle = \left[\frac{2\left(\bar{r}_{nl}(C_i)\cdot\bar{r}_{nl}(C_j)\right)^{1/2}}{\bar{r}_{nl}(C_i) + \bar{r}_{nl}(C_j)}\right]^{2l+3}. \quad (18)$$

Approximation (18) for calculating the probabilities of the SO processes (15) was analyzed in detail in [47] using the example of calculating the probabilities of the SO processes due to $L_3M_{45}M_{45}$ Auger and L_1-M_{45} radiative transitions in the xenon atom. It has been shown that using (18) in (15) gives good results with $k = 2$. Typical approximation errors $(15)-(18)$ at $k = 2$ amounted to approximately 10% for the most significant ejections, and the total probability of the SO processes.

    As mentioned above, the charge spectrum $P(q)$ of the final ions produced by the cascade decay of an inner vacancy is a set of probabilities for the formation of ions of all possible charges. All charge spectra must satisfy the normalization condition

$$P_{tot} = \sum_q P(q) = 1. \quad (19)$$

Since some low-probability branches of the decay tree have to be neglected in the calculations, for the calculated charge spectra $P^{calc}(q)$, especially those produced by complex decay cascades of deep vacancies, relation (19) is satisfied only approximately. In this study, when constructing the decay trees, we neglected all branches stemming from
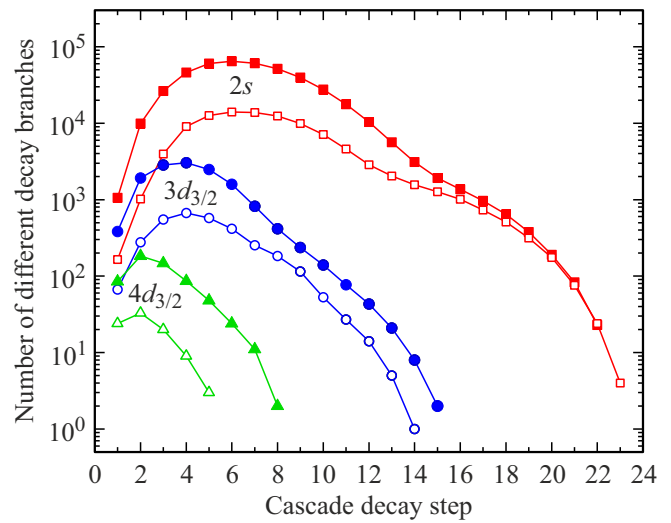
Figure 1. The number of different decay tree branches that appear at successive decay steps for the cascades with initial vacancies in the $2s$-, $3d_{3/2}$- and $4d_{3/2}$-subshells of the gold atom. Empty symbols — calculation without taking SO processes into account, solid symbols — calculation taking SO processes into account.

branching points whose probabilities to appear were less than 10^{-8}. The deviation of P^{calc}_{tot} from unity can serve a criterion for the accuracy of constructing a decay tree. Calculated charge spectra are renormalized to ensure the fulfillment of the condition (19):

$$P(q) = P^{calc}(q)/P^{calc}_{tot}. \quad (20)$$

   The average charges of the formed cascade ions are calculated by the formula

$$\langle q \rangle = \sum_q qP(q). \quad (21)$$

Results and Discussion

    Obtaining the charge spectra of final ions taking into account SO processes required large amounts of calculations. Fig. 1 shows the numbers of different ionic configurations arising at successive steps of cascade decays of vacancies in the $2s$-, $3d_{3/2}$- and $4d_{3/2}$-subshells of the gold atom. Shown are the data for the decay trees constructed without taking SO processes into account (empty symbols) and taking SO processes into account (solid symbols). Fig. 2 shows the total numbers of analyzed branches in the decay trees for the cascades with initial vacancies in all electron shells, starting from $1s$ and ending with $5p_{3/2}$. The shaded bars show the total number of branches in the trees built without SO processes, and the solid bars, the number of branches in the trees built taking SO processes into account. It can be seen from Figs. 1, 2 that taking into account additional monopole ejections significantly complicates the decay trees increasing the number of their branches by $50-64$ times for
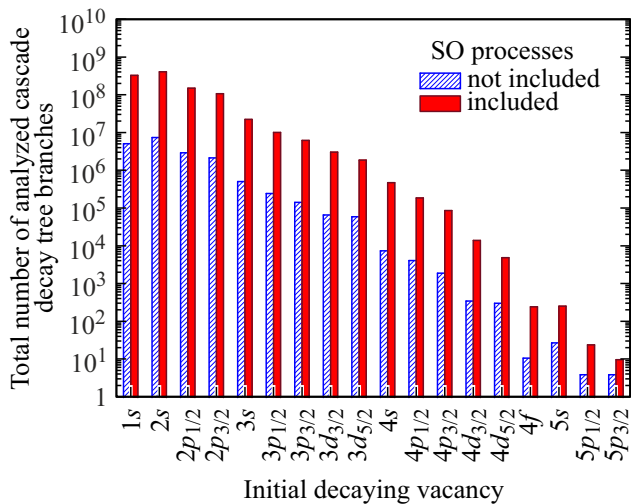
Figure 2. The total number of analyzed branches of the cascade decay trees in calculations without (shaded bars) and with (solid bars) SO-processes.
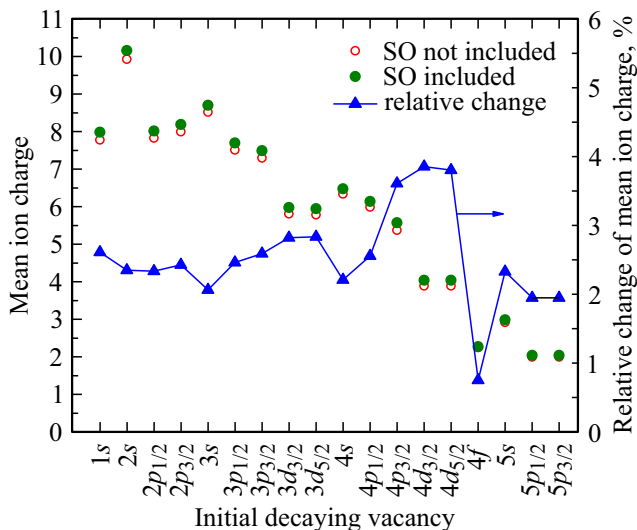
Figure 3. Average charges of cascade ions calculated without taking SO into account (open circles) and taking SO into account (solid circles) and relative changes in average ion charges upon allowance for the SO processes (triangles).

initial vacancies in *K*- and *L*-shells, by 32−47 times for initial vacancies in *M*-shell, by 16−63 times for vacancies in the *N*-shell and by 3−9 times for initial vacancies in the *O*-shell.

The most complicated is the decay tree of the 2*s*-vacancy. The number of its branches is $7.7 \cdot 10^6$ excluding SO processes and $4.3 \cdot 10^8$ if SO processes are included. The reason consists in the following. The fluorescence yield for the decay of a deeper 1*s* vacancy is 98%, with 78% coming from radiative transitions to the $2p_{1/2}^{-1}$ and $2p_{3/2}^{-1}$ states. Thus, at the first step of the decay of the $1s^{-1}$ state, the vacancy radiatively moves predominantly into the 2*p*-subshells, and the charge spectrum upon the decay of the 1*s* vacancy is

similar to the spectra on the decay of vacancies in the 2*p* subshells [40].

The probabilities of final ion formation in the cascade decay of vacancies in the *K*-, *L*-, *M*-, *N*- and *O*-shells of the gold atom calculated without taking into account, and taking into account the SO processes, are given in Tables 1−3. Calculated total probabilities (19) are also given there. The deviation from unity is maximal in the case of simulating the most complex decay of the 2*s*-vacancy taking into account SO processes, and is 0.04. In other cases, the deviations are smaller or negligible, which demonstrates sufficient accuracy in constructing the decay trees.

Fig. 3 shows the average ion charges calculated with and without allowance for the SO processes, as well as the relative changes in average ion charges after switching on the SO processes for cascades with initial vacancies in various electron subshells of the gold atom. It can be seen from the figure that, for most of the initial vacancies, the inclusion of SO leads to a rather insignificant relative increase in the average charge of the final ions by 2.0−2.8%. An exception is the decay of vacancies in the $4p_{3/2}$-, $4d_{3/2}$- and $4d_{5/2}$-subshells. For these, the relative increase in the average charge of the final ions is 3.6−3.9%. The smallest increase in the average ion charge when the SO processes are taken into account, equal to 0.8%, is observed for the decay of a vacancy in the 4*f*-subshell.

The presented results confirm the qualitative considerations [40] about the expected insignificant effect of the SO processes in heavy atoms. Despite the fact that at the first steps of the decay of inner vacancies, there are very numerous Auger transitions with the involvement of inner shells, for example, *LMM* Auger transitions, which formally lead to the appearance of an additional charge +1 inside the outer shells from which additional monopole electron ejections are possible, this charge is strongly screened by the electron density of a large number of electrons in the intermediate shells of the heavy atom. As a result, the relative change in the potential for the outer shells, which causes the SO processes, turns out to be small. The non-radiative transitions occurring at the middle and final steps of the cascade decay take place in highly ionized configurations containing a large number of vacancies, so the appearance of a new vacancy leads to only a relatively insignificant change in the potential for the outer shells.

These considerations are confirmed by direct calculations of the relative probabilities of the SO processes during the creation of an inner-shell vacancy depending on the atomic number, carried out in [39]. In that study, the authors calculated the ratios of the ionization probability of the n_0l_0-subshell with additional monopole excitation/ionization of an electron from the n_1l_1-subshell to the probability of single ionization of the n_0l_0-subshell per one n_1l_1-electron, $P_1(n_0l_0; n_1l_1)$. The dependences of $P_1(n_0l_0; n_1l_1)$ on the nuclear charge *Z* are monotonically decreasing and can be approximated by analytical functions:

$$P_1(n_0l_0; n_1l_1) = \frac{a}{(b-Z)^2}. \tag{22}$$

Table 1. Calculated probabilities of the formation of final Au^{q+} ions upon the cascade decay of vacancies in $1s$-, $2s$-, $2p_{1/2}$-, $2p_{3/2}$-, $3s$- and $3p_{1/2}$-subshells of the gold atom and the total probabilities of ion formation, P_{tot}^{calc}, calculated without taking into account (a) and taking into account (b) the SO-processes

q	Initial vacancy											
	$1s$		$2s$		$2p_{1/2}$		$2p_{3/2}$		$3s$		$3p_{1/2}$	
	a	b	a	b	a	b	a	b	a	b	a	b
1	0.0039	0.0033	4.E-5	3.E-5	0.0053	0.0044	0.0047	0.0039			0.0005	0.0004
2	0.0105	0.0097	0.0029	0.0025	0.0079	0.0079	0.0062	0.0062	0.0003	0.0003	0.0005	0.0001
3	0.0171	0.0162	0.0013	0.0012	0.0222	0.0208	0.0190	0.0177	0.0010	0.0009	0.0026	0.0024
4	0.0992	0.0839	0.0070	0.0062	0.1212	0.1027	0.1054	0.0891	0.0060	0.0051	0.0373	0.0308
5	0.0544	0.0606	0.0118	0.0104	0.0580	0.0682	0.0484	0.0575	0.0094	0.0086	0.0274	0.0281
6	0.1041	0.0873	0.0391	0.0313	0.0768	0.0683	0.0693	0.0606	0.0476	0.0365	0.1886	0.1443
7	0.0949	0.0987	0.0429	0.0421	0.0840	0.0846	0.0773	0.0770	0.0723	0.0658	0.1605	0.1693
8	0.1998	0.1914	0.1344	0.1217	0.1769	0.1687	0.1858	0.1730	0.3473	0.3092	0.3459	0.3380
9	0.1703	0.1679	0.1604	0.1506	0.1652	0.1601	0.1895	0.1808	0.3196	0.3199	0.1828	0.2065
10	0.1412	0.1488	0.2038	0.1952	0.1543	0.1590	0.1750	0.1817	0.1669	0.2020	0.0507	0.0718
11	0.0718	0.0851	0.1851	0.1830	0.0856	0.0972	0.0875	0.1035	0.0279	0.0466	0.0037	0.0081
12	0.0223	0.0311	0.1082	0.1191	0.0289	0.0380	0.0241	0.0350	0.0017	0.0048	6.E-5	0.0003
13	0.0075	0.0115	0.0601	0.0741	0.0103	0.0149	0.0067	0.0113	7.E-5	0.0003		4.E-6
14	0.0023	0.0036	0.0305	0.0422	0.0030	0.0046	0.0013	0.0025		3.E-6		
15	0.0006	0.0008	0.0108	0.0169	0.0005	0.0008	9.E-5	0.0002				
16	0.0001	0.0001	0.0017	0.0031	1.E-5	2.E-5						
17	1.E-5	4.E-6	0.0001	0.0003								
18			5.E-8	9.E-7								
P_{tot}^{calc}	0.9888	0.9771	0.9860	0.9577	0.9944	0.9829	0.9960	0.9865	0.9992	0.9959	0.9996	0.9981

Table 2. Calculated probabilities of the formation of final Au^{q+} ions upon the cascade decay of vacancies in $3p_{3/2}$-, $3d_{3/2}$-, $3d_{5/2}$-, $4s$-, $4p_{1/2}$- and $4p_{3/2}$-subshells of the gold atom and the total probabilities of ion formation, P_{tot}^{calc}, calculated without taking into account (a) and taking into account (b) the SO-processes

| q	Initial vacancy											
	$3p_{3/2}$		$3d_{3/2}$		$3d_{5/2}$		$4s$		$4p_{1/2}$		$4p_{3/2}$	
	a	b	a	b	a	b	a	b	a	b	a	b
1	0.0004	0.0003							2.E-5	1.E-5	2.E-5	1.E-5
2	0.0001	0.0001	0.0222	0.0213	0.0208	0.0200	0.0005	0.0004	0.0004	0.0004	0.0007	0.0007
3	0.0026	0.0024	0.0254	0.0239	0.0247	0.0233	0.0070	0.0067	0.0166	0.0155	0.0272	0.0254
4	0.0440	0.0363	0.2583	0.2199	0.2705	0.2303	0.0971	0.0834	0.1069	0.0948	0.1743	0.1546
5	0.0319	0.0329	0.1358	0.1550	0.1301	0.1523	0.1407	0.1349	0.1854	0.1658	0.2818	0.2511
6	0.2228	0.1705	0.1866	0.1631	0.1899	0.1643	0.2329	0.2135	0.3478	0.3121	0.4269	0.3773
7	0.1779	0.1915	0.1609	0.1730	0.1580	0.1716	0.3540	0.3375	0.2486	0.2840	0.0892	0.1734
8	0.3402	0.3390	0.1697	0.1852	0.1668	0.1826	0.1651	0.2101	0.0943	0.1229		0.0171
9	0.1512	0.1789	0.0383	0.0523	0.0367	0.0500	0.0027	0.0133	1.E-6	0.0043		0.0004
10	0.0283	0.0457	0.0029	0.0062	0.0026	0.0056		0.0002		0.0001		6.E-6
11	0.0006	0.0025	1.E-5	0.0001	1.E-5	8.E-5		2.E-6				
12		3.E-5										
P_{tot}^{calc}	0.9998	0.9988	0.9999	0.9994	0.9999	0.9995	1.0000	0.9999	1.0000	1.0000	1.0000	1.0000

Despite the fact that taking the SO processes into account changes the average final ion charge quite insignificantly, the probability distributions of ion production (charge spectra) can change quite noticeably in some cases. Fig. 4 shows the charge spectra produced by the decay of vacancies in some subshells of the gold atom, which illustrate the effect of taking the SO processes into account on their structure.

At present the opportunity of using compounds containing gold atoms and gold nanoparticles as radiosensitizers is intensively studied in the radiation therapy of oncological

Table 3. Calculated probabilities of the formation of final Au^{q+} ions upon the cascade decay of vacancies in $4d_{3/2}$-, $4d_{5/2}$-, $4f$-, $5s$-, $5p_{1/2}$- and $5p_{3/2}$-subshells of the gold atom and the total probabilities of ion formation, P_{tot}^{calc}, calculated without taking into account (a) and taking into account (b) the SO-processes

q	Initial vacancy											
	$4d_{3/2}$		$4d_{5/2}$		$4f$		$5s$		$5p_{1/2}$		$5p_{3/2}$	
	a	b	a	b	a	b	a	b	a	b	a	b
1					4.E-5	4.E-5			3.E-5	3.E-5	1.E-5	1.E-5
2	0.0097	0.0093	0.0096	0.0093	0.7463	0.7371	0.0802	0.0782	1.0000	0.9608	1.0000	0.9609
3	0.2254	0.2109	0.2257	0.2111	0.2537	0.2551	0.9198	0.8571		0.0391	0	0.0391
4	0.6278	0.5352	0.6284	0.5361		0.0076		0.0635		4.E-5		
5	0.1363	0.2187	0.1356	0.2183		0.0002		0.0015				
6	0.0008	0.0244	0.0007	0.0242				8.E-6				
7		0.0012		0.0010								
8		0.0003		5.E-6								
9		4.E-6										
P_{tot}^{calc}	1.0000	1.0000	1.0000	1.0000	1.0000	1.0000	1.0000	1.0000	1.0000	1.0000	1.0000	1.0000
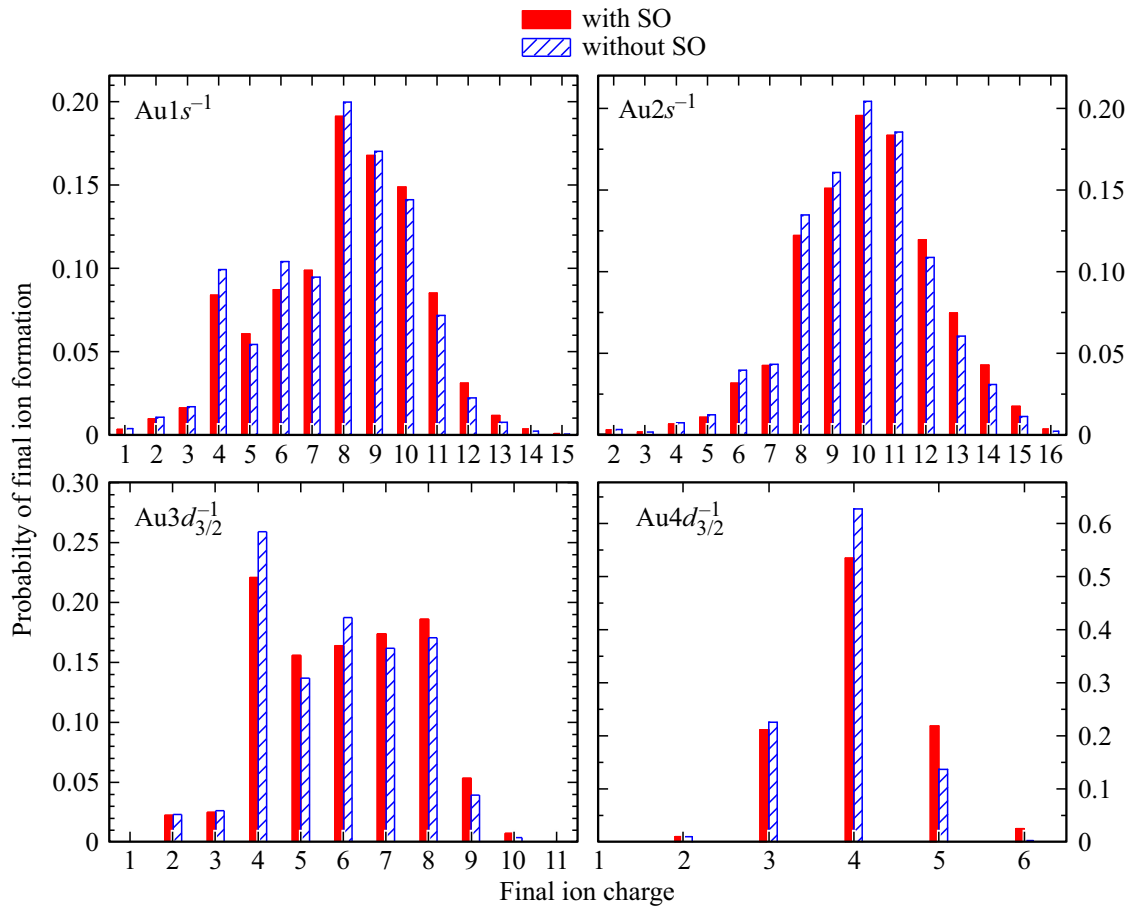
Figure 4. Charge spectra of final ions produced by the cascade decays of vacancies in $1s$-, $2s$-, $3d_{3/2}$- and $4d_{3/2}$-subshells of the gold atom. Shaded bars — calculation without taking into account the SO processes, solid bars — calculation with accounting for the SO processes.

diseases [50]; radiosensitizers are the objects capable of locally increasing the absorbed dose inside tumor tissues. This opportunity is due, firstly, to the large photoionization cross section of gold atoms and, secondly, to the ability of gold atoms to re-emit the energy of an absorbed photon together with cascade electrons and photons produced by

the cascade decay of an initial vacancy. Estimation of the energies carried away from an ionized radiosensitizer atom by cascade electrons E_{out}^{el} and photons E_{out}^{phot} is an important task in the development of radiation therapy strategies. In [25] E_{out}^{el} and E_{out}^{phot} are calculated for the iron atom in the decay of vacancies in K-, L- and M-shells.

It is of interest to study the effect of taking SO processes into account during the development of cascades on reemitted energies E_{out}^{el} and E_{out}^{phot}. It follows from general considerations that such an allowance should not significantly affect these quantities. In non-radiative, for example, Auger transitions, in the presence of an additional SO emission, the transition energy is only shared between the Auger electron and the SO electron, so that the total carried-away energy remains unchanged. As for radiative transitions, they do not lead to the creation of additional vacancies and a strong change in the potential, thus the probabilities of the SO processes are much smaller than in the case of Auger transitions [47]. However, it should be kept in mind that the inclusion of the SO branches modifies the cascade tree, which can affect the reemitted energies E_{out}^{el} and E_{out}^{phot}. Additional investigation is required for this issue.

Conclusion

The probabilities of the formation of final ions during the cascade decay of vacancies in the K-, L-, M-, N- and O-shells of the gold atom are calculated using the method of direct construction and analysis of the decay trees. Inclusion in the consideration of the SO processes caused by a change in the atomic potential during cascade transitions significantly (by dozens times) increases the number of branches of the decay tree and significantly increases computational costs. At the same time, taking the SO processes into account leads only to an insignificant (by $0.15-0.23e$) change in the average charge of the final ions. Meanwhile, the structure of the charge spectra of the final ions upon the decay of some initial vacancies changes, although slightly. It is suggested that taking the SO processes into account when calculating the energies reemitted by cascade electrons and photons, which are of interest in radiosensitization problems, will not play a significant role in the case of heavy radiosensitizing atoms.

Conflict of interest

The authors declare that they have no conflict of interest.

References

[1] M.O. Krause, M.L. Vestal, W.H. Johnston, T.A. Carlson. Phys. Rev., **133** (2A), A385 (1964).
DOI: 10.1103/PhysRev.133.A385
[2] T.A. Carlson, M.O. Krause. Phys. Rev., **137** (6A), A1655 (1965). DOI: 10.1103/PhysRev.137.A1655
[3] T.A. Carlson, M.O. Krause. Phys. Rev. Lett., **14** (11), 390 (1965). DOI: 10.1103/PhysRevLett.14.390
[4] M.O. Krause, T.A. Carlson. Phys. Rev., **149** (1), 52 (1966).
DOI: 10.1103/PhysRev.149.52
[5] T.A. Carlson, W.E. Hunt, M.O. Krause. Phys. Rev., **151** (1), 41 (1966). DOI: 10.1103/PhysRev.151.41
[6] M.O. Krause, T.A. Carlson. Phys. Rev., **158** (1), 18 (1967).
DOI: 10.1103/PhysRev.158.18
[7] T. Mukoyama. Bull. Inst. Chem. Res., Kyoto Univ., **63**, 373 (1985).
[8] T. Mukoyama, T. Tonuma, A. Yagishita, H. Shibata, T. Koizumi, T. Matsuo, K. Shima, H. Tawara. J. Phys. B, **20** (17), 4453 (1987).
DOI: 10.1088/0022-3700/20/17/023
[9] M.N. Mirakhmedov, E.S. Parilis. J. Phys. B, **21** (5), 795 (1988). DOI: 10.1088/0953-4075/21/5/010
[10] G. Omar, Y. Hahn. Phys. Rev. A, **44** (1), 483 (1991).
DOI:https://doi.org/10.1103/PhysRevA.44.483
[11] G. Omar, Y. Hahn. Z. Phys. D, **25** (1), 41 (1992).
DOI: 10.1007/BF01437518
[12] G. Omar, Y. Hahn. Z. Phys. D, **25** (1), 31 (1992).
DOI: 10.1007/BF01437517
[13] A.G. Kochur, A.I. Dudenko, V.L. Sukhorukov, I.D. Petrov. J. Phys. B, **27** (9), 1709 (1994).
DOI: 10.1088/0953-4075/27/9/011
[14] A.G. Kochur, V.L. Sukhorukov, A.J. Dudenko, P.V. Demekhin. J. Phys. B, **28** (3), 387 (1995).
DOI: 10.1088/0953-4075/28/3/010
[15] A. El-Shemi, Y. Lofty, I. Reiche, G. Zschornack. Radiat. Phys. Chem., **49** (4), 403 (1997).
DOI: 10.1016/S0969-806X(96)00178-8
[16] A.H. Abdullah, A.M. El-Shemi, A.A. Ghoneim. Radiat. Phys. Chem., **68** (5), 697 (2003).
DOI: 10.1016/S0969-806X(03)00433-X
[17] V. Jonauskas, L. Partanen, S. Kučas, R. Karazija, M. Huttula, S. Aksela, H. Aksela. J. Phys. B, **36** (22), 4403 (2003).
DOI: 10.1088/0953-4075/36/22/003
[18] A.M. El-Shemi. Jpn. J. Appl. Phys., **43** (5R), 2726 (2004).
DOI: 10.1143/JJAP.43.2726
[19] A.M. El-Shemi. Can. J. Phys., **82** (10), 811 (2004).
DOI: 10.1139/p04-045
[20] Y.A. Lotfy, A.M. El-Shemi. Symmetry, Integr. Geom. Methods Appl., **2**, 015 (2006). DOI: 10.3842/SIGMA.2006.015
[21] A.M. Mohammedein, A.A. Ghoneim, K.M. Kandil, I.M. Kadad. AIP Conf. Proc., **1202**, 213 (2010).
DOI: 10.1063/1.3295600
[22] A.P. Chaynikov, A.G. Kochur, V.A. Yavna. Opt. i spektr., **119** (2), 179 (2015) (in Russian).
DOI: 10.7868/S003040341508005X

[A.P. Chaynikov, A.G. Kochur, V.A. Yavna. Opt. Spectrosc., **119** (2), 171 (2015). DOI: 10.1134/S0030400X15080056].

[23] X.L. Wang, B.X. Liu, G.H. Zhang, P.Y. Wang, L.W. Liu, X.Y. Li. J. Electron Spectros. Relat. Phenomena., **250**, 147083 (2021). DOI: 10.1016/j.elspec.2021.147083

[24] V.L. Jacobs, J. Davis, B.F. Rozsnyai, J.W. Cooper. Phys. Rev. A, **21** (6), 1917 (1980). DOI:10.1103/PhysRevA.21.1917

[25] A.G. Kochur, A.P. Chaynikov, A.I. Dudenko, V.A. Yavna. JQSRT, **286**, 108200 (2022).
DOI: 10.1016/j.jqsrt.2022.108200

[26] S. Kučas, P. Drabužinskis, A. Kynienė, Š. Masys, V. Jonauskas. J. Phys. B, **52** (22), 225001 (2019).
DOI: 10.1088/1361-6455/ab46fa

[27] S. Kučas, P. Drabužinskis, V. Jonauskas. At. Data Nucl. Data Tables, 135−136, 101357 (2020).
DOI: 10.1016/j.adt.2020.101357

[28] G. Omar, Y. Hahn. Phys. Rev. A, **43** (9), 4695 (1991).
DOI: 10.1103/PhysRevA.43.4695

[29] S. Fritzsche, P. Palmeri, S. Schippers. Symmetry (Basel), **13** (3), 520 (2021). DOI: 10.3390/sym13030520

[30] S. Kučas, R. Karazija, A. Momkauskaitė. Astrophys. J., **750** (2), 90 (2012). DOI: 10.1088/0004-637X/750/2/90

[31] C. Gerth, A.G. Kochur, M. Groen, T. Luhmann, M. Richter, P. Zimmermann. Phys. Rev. A, **57** (5), 3523 (1998).
DOI: 10.1103/PhysRevA.57.3523

[32] A. El-Shemi, Y. Lofty, G. Zschornack. J. Phys. B, **30** (2), 237 (1997). DOI: 10.1088/0953-4075/30/2/017

[33] A. El-Shemi, A. Ghoneim, Y. Lotfy. Turk. J. Phys., **27**, 51 (2003).
URL: https://journals.tubitak.gov.tr/physics/vol27/iss1/5

[34] A. El-Shemi. Turk. J. Phys., **28**, 229 (2004).
URL: https://journals.tubitak.gov.tr/physics/vol28/iss4/3/

[35] A.M. El-Shemi, Y.A. Lotfy. Eur. Phys. J. D, **32** (3), 277 (2005).
DOI: 10.1140/epjd/e2005-00003-3

[36] V.P. Sachenko, V.F. Demekhin. Sov. Phys. JETP, **49** (3), 765 (1965).

[37] T.A. Carlson, C.W. Nestor, T.C. Tucker, F.B. Malik. Phys. Rev., **169** (1), 27 (1968). DOI: 10.1103/PhysRev.169.27

[38] T. Mukoyama, K. Taniguchi. Phys. Rev. A, **36** (2), 693 (1987).
DOI: 10.1103/PhysRevA.36.693

[39] A.G. Kochur, A.I. Dudenko, D. Petrini. J. Phys. B, **35** (2), 395(2002). DOI: 10.1088/0953-4075/35/2/315

[40] A.P. Chaynikov, A.G. Kochur, A.I. Dudenko, I. Petrov, V.A. Yavna. Phys. Scr., **98** (2), 025406 (2023).
DOI: 10.1088/1402-4896/acb407

[41] F. von Busch, J. Doppelfeld, C. Gunther, E. Hartmann. J. Phys. B, **27** (11), 2151 (1994).
DOI: 10.1088/0953-4075/27/11/011

[42] R. Kau, I.D. Petrov, V.L. Sukhorukov, H. Hotop. Z. Phys. D, **39** (4), 267 (1997). DOI: 10.1007/s004600050137

[43] S.T. Perkins, D. Cullen, M.H. Chen, J. Rathkopf, J. Scofield, J.H. Hubbell. *Tables and Graphs of Atomic Subshell and Relaxation Data Derived from the LLNL Evaluated Atomic Data Library (EADL), Z=1-100*, Vol. UCRL-50400 (US Department of Energy, Office of Scientific and Technical Information, United States, 1991).

[44] D.L. Walters, C.P. Bhalla. Phys. Rev. A, **3** (6), 1919 (1971).
DOI: 10.1103/PhysRevA.3.1919

[45] V.G. Yarzhemsky, A. Sgamellotti. J. Electron Spectros. Relat. Phenomena, **125** (1), 13 (2002).
DOI: 10.1016/S0368-2048(02)00042-7

[46] A.G. Kochur, A.I. Dudenko, I.D. Petrov, V.F. Demekhin. J. Electron Spectros. Relat. Phenomena, **156**−**158**, 78 (2007). DOI: 10.1016/j.elspec.2006.11.033

[47] A.G. Kochur *Protsessy raspada vakansiy v glubokikh elektronnykh obolochkah.* (in Russian). Avtoref. dis. dokt. fiz.-mat. nauk (Rostov-on-Don, 1997) (in Russian).
URL: https://search.rsl.ru/ru/record/01000199628

[48] R. Karazija. *Sums of Atomic Quantities and Mean Characteristics of Spectra* (Mokslas, Vilnius, 1991).

[49] S. Kučas, R. Karazija. Phys. Scr., **47** (6), 754 (1993).
DOI: 10.1088/0031-8949/47/6/012

[50] Y. Liu, P. Zhang, F. Li, X. Jin, J. Li, W. Chen, Q. Li. Theranostics, **8** (7), 1824 (2018). DOI: 10.7150/thno.22172

Translated by E.Potapova